Sensors and Actuators A 224 (2015) 36–42

Contents lists available at ScienceDirect

Sensors and Actuators A: Physical

journal homepage: www.elsevier.com/locate/sna

Self-similar design for stretchable wireless *LC* strain sensors

YongAn Huang[a,*,1], Wentao Dong[a,1], Tao Huang[a], Yezhou Wang[a], Lin Xiao[a], Yewang Su[b,c,d], Zhouping Yin[a,**]

[a] State Key Lab of Digital Manufacturing Equipment and Technology, School of Mechanical Science and Engineering, Huazhong University of Science and Technology, 430074 Wuhan, PR China
[b] State Key Laboratory of Nonlinear Mechanics, Institute of Mechanics, Chinese Academy of Sciences, Beijing 100190, PR China
[c] Department of Civil and Environmental Engineering, Northwestern University, Evanston, IL 60208, USA
[d] Department of Mechanical Engineering, Northwestern University, Evanston, IL 60208, USA

ARTICLE INFO

Article history:
Received 6 August 2014
Received in revised form
24 December 2014
Accepted 6 January 2015
Available online 19 January 2015

Keywords:
Stretchable electronics
Wireless strain sensor
Artificial skin
Self-similar structure

ABSTRACT

Stretchable sensors provide a foundation for applications that exceed the scope of conventional device technologies due to their unique capacity to integrate with soft materials and curvilinear surfaces. This article presents the implementation and characterization of a large-area stretchable wireless *RF* strain sensor, operating at around 760 MHz, based on the concept of self-similar design. It has an electrical *LC* resonant circuit formed by a self-similar inductor coil and a capacitor to facilitate passive wireless sensor. The inductance of the wireless sensor varies with the elongation of the PDMS substrate, so is the resonance frequency of the sensor that is detected using an external coil linked to a vector network analyzer. Finite element modeling was used in combination with experimental verification to demonstrate that the wireless strain sensor with 300 μm width can be stretched up to 40%. Self-similar structured coil incorporating variable inductance has been implemented to monitor the strain of artificial skin. Strain response of the stretchable wireless sensor has been characterized by experiments, and demonstrates high strain responsivity about 33.7 MHz/10%, which confirms the feasibility of strain sensing for biomedical and wearable applications.

1. Introduction

Stretchable sensors have the potential to open up new opportunities, particularly for large-area wearable devices that can conform to a curved surface or to bending, twisting and stretching while in use with deformable parts [1,2]. Stretchable wireless sensors featuring variant electrical characteristics in response to mechanical deformation may offer an effective solution to self-contained large-area strain sensors [3]. There are many types of strain gauges existing, such as piezoresistive materials (Si [4], carbon nanotube [5], carbon-black [6].), and piezoelectric material (lead zirconate titanate (PZT) [7], zinc oxide (ZnO) [8], poly(vinylidene fluoride, PVDF) [9,10]) on a flexible or stretchable substrate. Continuous artificial skin strain monitoring is a consistent need for biological applications, e.g. heartbeat rates, body temperature, blood pressure, mechanical strains or motion [11]. However, the rocketing demands on wireless wearable sensors capable of measuring repeated high strains over large-area body surfaces or intense body motion are presently challenging technologies of strain sensor due to their poor elasticity and insufficient active areas [12].

Stretchable, biological integrated sensors for wireless reception/transmission were reported, which involve *RF* energy harvesting [13], communication and strain monitoring [14,15]. A novel micromachined passive sensor with wireless antenna is designed to measure the pressure information which consists of a tuned circuit and the sensors show a shift in their resonant frequency around at 10 *GHz* in response to changing pressure [16]. Stretchable wireless strain sensors with variable capacitor or inductor are able to accomplish continuous and faithful noncontact body surfaces strain measurements [17]. In wireless *RF* active sensing, the power transfer, size, and cost are critical concerns [18,19]; however, the passive sensing approaches have relatively dexterous design considerations [20,21]. A capsulated sensor with an electrical *LC* tank resonant circuit was implanted to the anterior chamber for pressure monitoring [22,23]. Wireless strain sensors have been developed with the *LC* resonant circuit concept for various sensing applications, including body surface monitoring,

* Corresponding author. Tel.: +86 13545354545; fax: +86 2787543072.
** Corresponding author.
E-mail addresses: yahuang@hust.edu.cn (Y. Huang), yinzhp@mail.hust.edu.cn (Z. Yin).
[1] These authors contributed equally to this work.

http://dx.doi.org/10.1016/j.sna.2015.01.004
0924-4247/

transcutaneous, ophthalmic and intracranial pressure monitoring [24–26]. Stretchable serpentine design with *LC* resonators for wireless determination of strain properties of skin surface was reported [27]. These devices serve as excellent examples of such wireless passive pressure sensors for the continuous measurement of physiological parameters. Despite successful wireless pressure sensing demonstration, it is urgent to improve the deformability of wireless strain sensor with an *LC* resonant circuit. Currently two approaches are utilized to fabricate stretchable inorganic electrical circuit: (1) patterned thin film on prestrained substrate to generate nonplanar buckled film with stretchability [28,29] and (2) serpentine film on stretchable substrate whose stretchability is largely reduced at the case of interfacial bonding [30,31].

We propose a stretchable wireless sensor based on self-similar design for large-area cutaneous strain/pressure monitoring. It is composed of self-similar ribbon (Cu film) using as an inductor, and a capacitor, which are formed an *LC* resonant circuit. The self-similar serpentine structure is designed to improve the stretchability, and the inductance is variable with the deformation of the wireless coil under stretching. The relationship between the resonance frequency and the applied strain is found based on experiments that the deformation of soft object can be determined from the resonance frequency. The stretchable wireless strain sensors are fabricated by the combination of photolithography and wet etching approach. The stretchability is validated by finite element simulations in combination with experiments. The rest of the paper is organized as follows: Section 2 describes design and fabrication of wireless strain sensor. Section 3 shows the comparison between the finite element simulations and the experiment results. Section 4 analyzes the relationship between the variant inductance of the wireless strain sensor and the applied strain. Section 5 presents measurement results of wireless strain sensor with different stretched lengths and sensitivity analysis of the wireless strain sensor is given.

2. Self-similar design and fabrication of wireless *LC* strain sensor

The stretchability of *LC* circuit with large cross-section width is limited, meanwhile the sensitivity should be high enough to sensing the external deformation. We design stretchable coil based on self-similar serpentine structure, which can provide design solution to meet the requirement of large deformation, large area, and high sensitivity of the wireless sensor for continuous strain monitoring. The core is to design an electrical coil with high

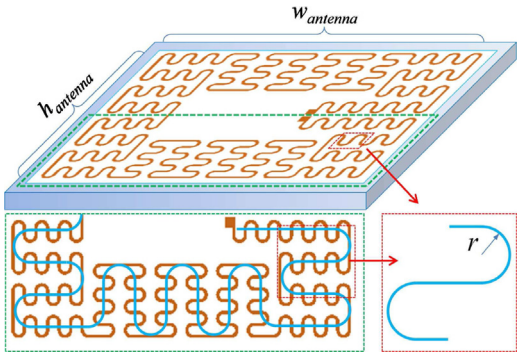

Fig. 1. The designed geometry of the fractal antenna with self-similar serpentine structure.

stretchability, and the electrical coil simultaneously has the capability of tuning the inductance, capacitance, or resistance by the applied strain. Design sketch of self-similar serpentine structure is shown in Fig. 1. The self-similar design follows from iteratively applying this basic geometry, beginning with a serpentine unit cell as illustrated schematically. The self-similar geometry leads to hierarchical bending physics that ensures ultra-low strains in the materials, even under extreme stretching. It will provide an effective way to transfer print the stiff inorganic structures with low strains to the soft bio-materials or organic materials. It is able to shrink the overall dimension of the coil, and then tune the inductance, capacitance, and resistance of coil to enhance the total performance. The size of wireless coil is $h_{antenna}$ = 30.5 mm and $w_{antenna}$ = 43.7 mm (central axis) with w_{line} =100–500 μm line width and 10 μm thickness, the whole length is 458.5 mm, the radii of the first and second level serpentines are r_1 = 2 mm and r_2 = 0.75 mm (central axis).

Additionally, this kind of serpentine antennas, such as meander and zig–zag shaped antennas [32], can reduce the capability in antenna size. Initially, the fractal concept in stretchable electronics is presented to merely improve the deformability, by using thin films of hard electronic materials patterned in deterministic fractal motifs and bonded to elastomers [33]. Self-similar design of stretchable electronics was reported in the literature in the form of a self-similar serpentine configuration, which is used to achieve >300% system stretchability for a lithium-ion battery [34].

Wet etching fabrication processes for the fractal wireless coil (an electrical *LC* resonant circuit) are demonstrated in Fig. 2 [35]. The critical steps are involved as follows. (a) One Cu film with ~10 μm

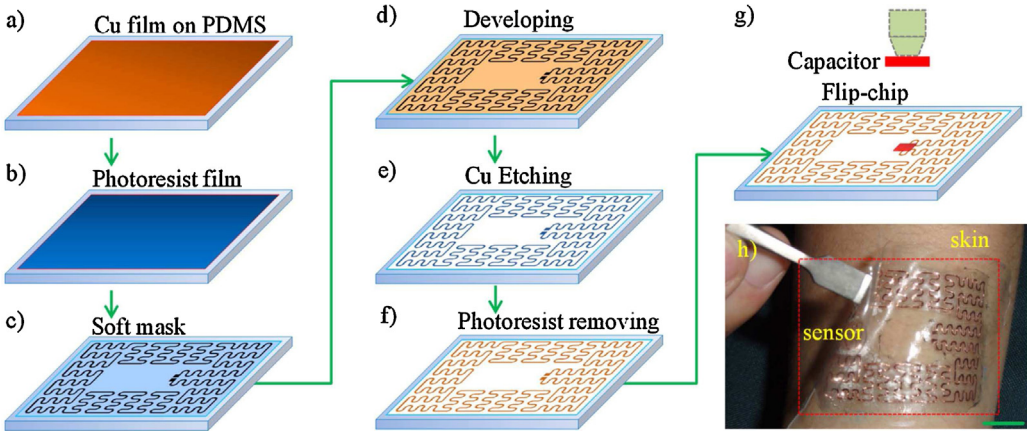

Fig. 2. Main fabrication steps for the stretchable wireless sensors: (a) a piece of Cu film bonded on PDMS; (b) spin coating a 2 μm thick photoresist film onto copper foil; (c) placing the soft mask onto photoresist film closely, then transfer them into the exposure machine; (d) the stretchable substrate with photoresist will put into the developing powder solution (20 g/2 l); (e) the fractal antenna is put on etchant solution (50 g/200 ml) about 15 min; (f) the photoresist film mold is released by powder solution (20 g/200 ml); (g) flip-chip bonding the capacity with the fractal antenna and (h) self-similar coil on skin. The bar denotes 10 mm.

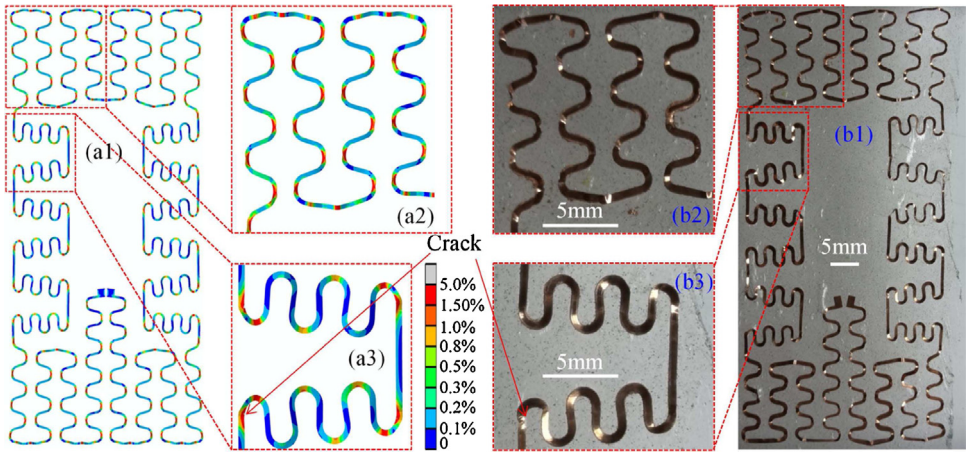

Fig. 3. Comparison between the FEA simulation and experiment results of wireless strain sensor stretched 40%: (a) the distribution of maximum principal strain by FEA and (b) the optical images of the deformation of wireless strain sensors.

thickness is bonded to ~200 μm thickness PDMS substrate. (b) The surface of the copper is spin-coated with the photoresist with the thickness of less than 2 μm. (c) The soft mask film with self-similar wireless coil pattern is used to control the penetration of the ultraviolet (UV). The mask-on-photoresist system is moved into the exposure machine under UV to be exposed about 5–10 min. (d) The stretchable substrate with photoresist will put into the developing powder solution (20 g/2 l), and the photoresist without UV irradiating would disappear. The pattern is transferred to the photoresist film. (e) The developed Cu film is put into etchant solution (50 g/200 ml) about 15 min. When the copper without photoresist film protecting is etched by the etchant solvent, the structured film for fractal coil with self-similar structure is formed. (f) The photoresist film mold would be released by acetone solution from the copper coil, and the fractal Cu coil is cleaned. (g) The selected capacity C_s was mounted onto wireless coil using flip-chip process. Anisotropic conductive film is used to bond the capacity and wireless coil together. The stretchable wireless coil can be stretched by external force adding to the end of PDMS substrate. The fabricated self-similar wireless coil is mounted on skin, as shown in Fig. 2h. It can be used to monitor the strain of the skin by an external wireless coil linked with a vector network analyzer.

3. Structural stretchability of the fractal antenna

The deformability is the distinct advantage of self-similar coil over other coil. Several factors should be considered in self-similar design, including the stretchability and stiffness of self-similar design, the controlling of deformation mode, the coupling relationship between deformation and electrical frequency, and the integration degree of coil. Additionally, we have proved that the cross-section dimension plays a critical role in controlling deformation mode, such as in-surface and out-of-surface buckling [9]. When the thickness becomes larger than the line width w_{line}, the serpentine structure can avoid out-of-surface wrinkling. The deformation mechanisms of self-similar structures ensure low levels of strain in the materials before they become straight structures. The mechanism of stretching self-similar structure can be mainly attributed to the tremendous reduction of stiffness in the second order structure compared to the first order one [36]. The self-similar serpentine structures can be stretched elastically by optimizing the width and the curvature radius. The stretchability can be extended largely only by increasing the length of the interconnection, which improves the design flexibility of stretchable devices [37]. The stretchability is evaluated quantitatively by finite element analysis (FEA) using the commercial package *ABAQUS*6.10. In addition to the self-similar shape, the cross-section width w_{line} plays an important role in controlling the stretchability. The self-similar structure with $w_{line} = 300$ μm is considered as the example of the mechanics analysis. Fig. 3 shows the comparison between the FEA results and the optical images of experiment, where the self-similar antenna is stretched with 40%. The FEA results illustrate the principal strain distribution, as well as two local enlarged figures (Fig. 3a2 and a3). Optical images show the structural deformation, as well as two local enlarged optical graphs (Fig. 3b2 and b3). The FEA simulation agrees well with the experimental results in the respect of structural deformation. The FEA results show the distribution of maximum principal strain, and the maximum values appear at Part a2 and a3. It can be proved indirectly that the largest out-of-plane buckling appears at corresponding position (Fig. 3b2 and b3). The wireless coil could work when it is stretched to 40%. The simulation results show that the strain of most part is smaller than 1.0%, and the maximum strain reaches the crack strain 5%.

When the PDMS substrate releases, some parts of the wireless coil deform out of plane. It can provide a guideline to design the wireless fractal coil through FEM simulation, and also provides one effective method to reduce maximum strain of wireless fractal coil and to improve the stretchability of wireless fractal coil. Significantly, the self-similar design outperforms the conventional serpentine system in stretchability. Self-similar design with high stretchability will improve the practical applicability, especially in functional devices with high areal capacity, which requires large coverage of the active regions.

Fig. 4 shows the maximum strain ε_{max} of the wireless coil versus the applied strain. The maximum value in the self-similar antenna is a linear, monotonous, increasing function of the applied strain $\varepsilon_{applied}$ (when the maximum strain ε_{max} does not reach the crack strain 5%). The crack length w_{crack} of the wireless coil in the width direction is the place where the strain of the coil is larger than 5% (the critical crack value of the Cu). The self-similar structure with 300 μm width is broken when stretched up to 40%, which is validated by simulation and experiment. The FEA simulation shows that the stretchability is not a monotonous function of the cross-section width w_{line}.

4. Strain-induced tunable inductance

Fig. 5 is the schematic diagram of the principle of wireless *LC* sensing system. The strain sensor can exchange energy with the external coil linked to network analyzer, to detect the resonance

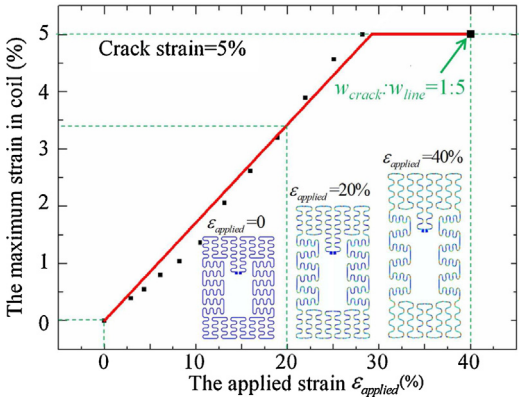

Fig. 4. Dependence of Cu strain on the applied strain, and the stretchability related with the coil width.

frequency. The resonance frequency of the electrical *LC* circuit is represented as [38]:

$$f_{resonant} = \frac{1}{2\pi}\sqrt{\frac{1}{L_sC_s} - \frac{R_s^2}{L_s^2}} \cong \frac{1}{2\pi\sqrt{L_sC_s}} \quad \text{when} \quad R_s^2 << \frac{L_s}{C_s} \tag{1}$$

where L_s, C_s and R_s are the inductance, capacitance, and resistance of the sensor, respectively.

The inductance of the self-similar wireless coil varies with the applied strain on the PDMS substrate, which leads to the change of the resonance frequency. The equivalent circuit of the wireless sensor contains a *RLC* resonant circuit with variant inductance, as shown in Fig. 5. The relationship between the strain and resonance frequency determines the sensitivity between the stretchability and the wireless system. Electricity parameters resistance R_s, inductance L_s and capacitance C_s of the stretchable wireless strain sensor have large influence on the equivalent impedance value $Zeq(\omega)$ which can be written as

$$Zeq = R_s + j2\pi f_{scan}L_s + \frac{1}{j2\pi f_{scan}C_s} \tag{2}$$

The resistance R_s of sensor is almost unchanged with repetition measurement for different applied strains since the cross-section and length keep nearly invariable during stretching. In the stretchable wireless *LC* sensor, a capacitance C_s is selected to match the inductance L_s. Compared to the selected chip capacitance, the parasitic capacitance of the wireless coil can be negligible. The capacitance C_s for the wireless sensor also keeps invariant.

It can be observed from Eq. (2) that the equivalent impedance value $Zeq(\omega)$ is deeply related with inductance L_s and scanning frequency f_{scan}. The inductance value L_s is influenced by the deformation of the fractal coil with self-similar structure. The inductance values L_s are measured by an Impedance Analyzer (E4982A LCR,

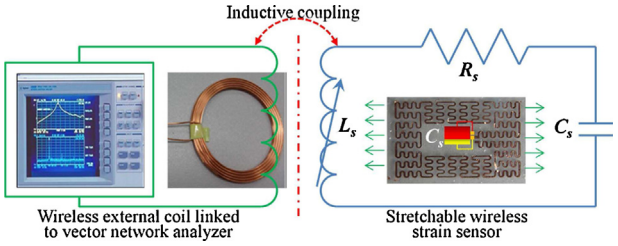

Fig. 5. Schematic diagram of principle of wireless *LC* strain sensor, and the equivalent circuit of wireless strain sensor with variant inductance (optical image of the stretchable wireless sensor based on self-similar design).

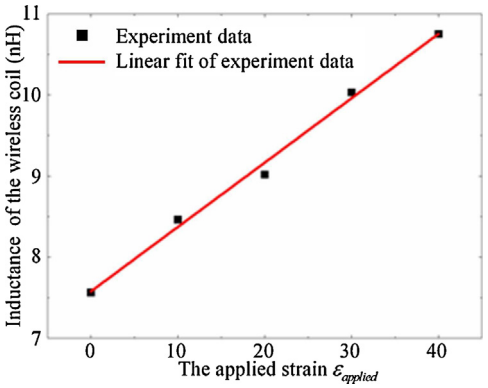

Fig. 6. Experiment data and linear fit graph between the inductance value and strain of wireless sensor.

Agilent Technologies) When the sensor is stretched up to 0, 10%, 20%, 30% and 40%. Linear fitting for the inductance value L_s and the strain $\varepsilon_{applied}$ is shown as Eq. (3). L_s monotonously increases with the applied strain $\varepsilon_{applied}$. Fig. 6 shows experimentally the relationship between the inductance value L_s and the applied strain $\varepsilon_{applied}$.

$$L_s(\varepsilon_{applied}) = a + b\varepsilon_{applied} = 7.578 + 7.940\varepsilon_{applied} \tag{3}$$

Submit Eq. (3) into Eq. (1), one can get the resonance frequency as

$$f_{resonant}(\varepsilon_{applied}) = \frac{1}{2\pi(7.578 + 7.940\varepsilon_{applied})C_s} \tag{4}$$

The inductance of the wireless coil is measured in 10% strain increments from 0 to 40%. Substitute the inductance measurement value into Eq. (1), respectively, and the resonant frequency of the wireless sensor can be computed. Relationship between the computed resonant frequency and strain is shown as the scattered points in Fig. 8. A continuous line in Fig. 8 is plotted with Eq. (4). Fig. 7 illustrates the resonance frequency $f_{resonant}(\varepsilon_{applied})$ of the stretchable wireless sensor related with the applied strain $\varepsilon_{applied}$. With the increasing of the applied strain $\varepsilon_{applied}$, the inductance L_s monotonously increases, but the resonance frequency $f_{resonant}$ monotonously decreases. The resonance frequency is sensitive to the applied strain, based on which the strain can be measured by the resonance frequency.

Combine Eq. (3) with Eq. (2), the equivalent impedance value $Zeq(\omega)$ can be written as

$$Zeq(\varepsilon_{applied}) = R_s + j2\pi f(7.578 + 7.940\varepsilon_{applied}) + \frac{1}{j2\pi fC_s} \tag{5}$$

The equivalent impedance value $Zeq(\omega)$ of the wireless strain sensor is determined by parameter inductance L_s and scanning

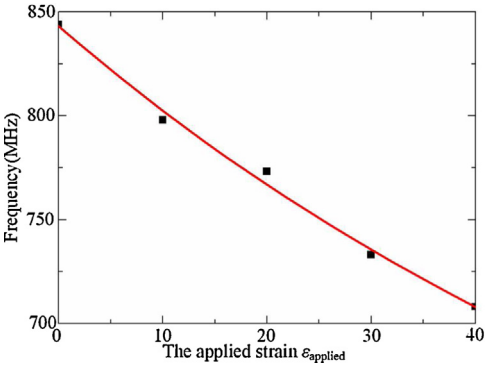

Fig. 7. The resonance frequency $f_{resonant}(\varepsilon_{applied})$ versus strain of the wireless sensor.

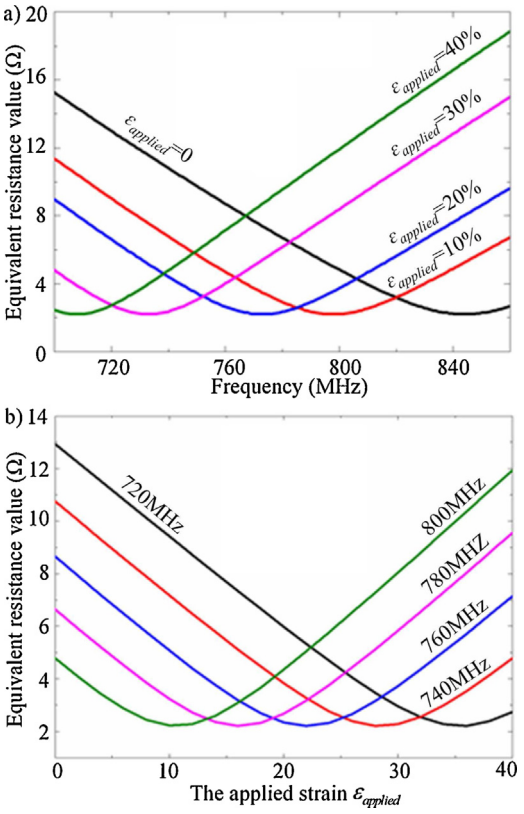

Fig. 8. (a) Equivalent resistance value versus scanning frequency with different applied strains and (b) equivalent resistance value versus strain of wireless strain sensor with different desired frequency.

frequency f_{scan}. Fig. 8a shows the relationship between equivalent impedance value $Zeq(\omega)$ and scanning frequency, where the desired strains is applied on the substrate from 0 to 0.4 with 0.1 interval. It illustrates for a given a desired strain $\varepsilon_{applied}$ that the equivalent resistance is the minimal value in the scanning frequency interval, and the minimal value decreases with the applied strain. The desired resonance frequency appears at the minimum resistance value of wireless sensor system from 720 to 800 MHz with 20 MHz interval. Additionally, the fractal Cu structure can be utilized as a mechanically tunable antenna. Fig. 8b demonstrates that the relationship between the equivalent impedance value and the applied strain. The desired resonance frequency can be gotten though stretching the wireless sensor. Namely, if one can stretch the stretchable fractal Cu coil as a mechanically tunable antenna to get the desired scanning frequency.

5. Experimental platform and sensitivity analysis

The measurement setup in Fig. 5 consists of a stretchable wireless strain sensor clamped on stretcher. The right frame depicts the stretchable wireless sensor with variable inductance and a common captivity. The wireless sensor is stretched to the resonance frequency continuously. This frequency is detected using an external coil connected to the vector network analyzer. The wireless reading range of the sensor is about 1 m in the stretched state. Strain differences were generated by stretching the PDMS substrate through a customized clamp (with 0.1 mm tuning resolution) to a controllable deformation device. The external reader coil was aligned above the stretchable wireless sensor on the same axis using a manipulation stage. As long as the impedance phase dip is detected in the frequency scan, the resonance frequency is accurately characterized. If the sensor implant has strain-sensitive electrical components,

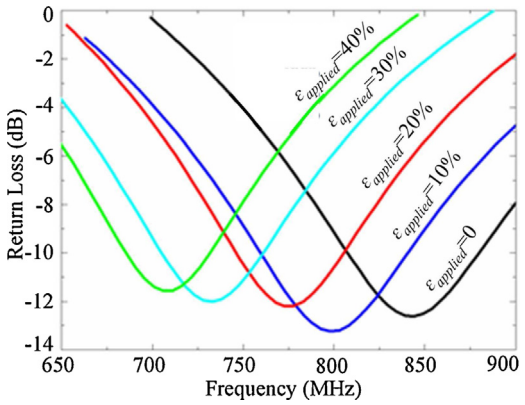

Fig. 9. Overlay plot of measured return loss versus scanning frequency with different stretched lengths bonded onto the artificial skin.

its resonance frequency will be shifted based on external strain variation.

The shape of wireless coil changes with the stretching of PDMS substrate. The sensitivity is of importance for the wireless *LC* sensor. When the embedded metal components are away from the bottom substrate, it leads to a decrease in the inductance and an increase in the resonance frequency. The normalized shifted resonance frequency can be written as

$$\frac{f_{resonant\_0}}{f_{resonant}} = \frac{1/2\pi\sqrt{L_sC_s}}{1/2\pi\sqrt{(L_s+\Delta L)C_s}} = \sqrt{1+\frac{\Delta L}{L_s}} = \sqrt{1+\alpha\Delta\varepsilon_{applied}} \tag{6}$$

where $f_{resonant\_0} = f_{resonant}(\varepsilon_{applied} = 0)$, ΔL is the increment of inductance resulted from the structural deformation, $\Delta\varepsilon_{applied}$ is the increment of applied strain, and α is determined by the material properties, physical dimensions of the device and external strain $\varepsilon_{applied}$. As $\Delta\varepsilon_{applied}$ changes, the resonance frequency of the stretchable wireless sensor also changes.

Submit Eq. (3) into Eq. (6), one can get

$$\alpha = \frac{b}{a + b\varepsilon_{applied}} \tag{7}$$

It can be noted that α is related with the applied strain, and can be extended based on Taylor series. When $\Delta\varepsilon_{applied}$ is small enough, Eq. (6) can be further derived as

$$\begin{aligned}\frac{f_{resonant\_0}}{f_{resonant}} &= \sqrt{1+\alpha\Delta\varepsilon_{applied}} \\ &= 1 + \frac{1}{2}\alpha\Delta\varepsilon_{applied} - \frac{1}{8}(\alpha\Delta\varepsilon_{applied})^2 + \cdots \\ &\cong 1 + \frac{1}{2}\alpha\Delta\varepsilon_{applied}\end{aligned} \tag{8}$$

The sensitivity of the wireless sensor can be shown as

$$S = \frac{\partial(f_{resonant\_0}/f_{resonant})}{\partial\Delta\varepsilon_{applied}} = \frac{1}{2}\frac{b}{a + b\varepsilon_{applied}} \tag{9}$$

The sensitivity is related with the applied strain since is determined by the applied strain. Supposed that the applied strain is equal to zero, and one can get $S|_{\varepsilon=0} = 5239$ ppm/1%.

Fig. 9 shows the measurement results of return loss with the operation frequency, in different stretched status (from 0 to 40%) of wireless sensor bonded onto the artificial skin. Operation frequency shift with applied strain in a highly sensitive and kinematics controlled manner, and the return losses are all smaller than −10 dB in experiment results, which successfully verified the feasibility of

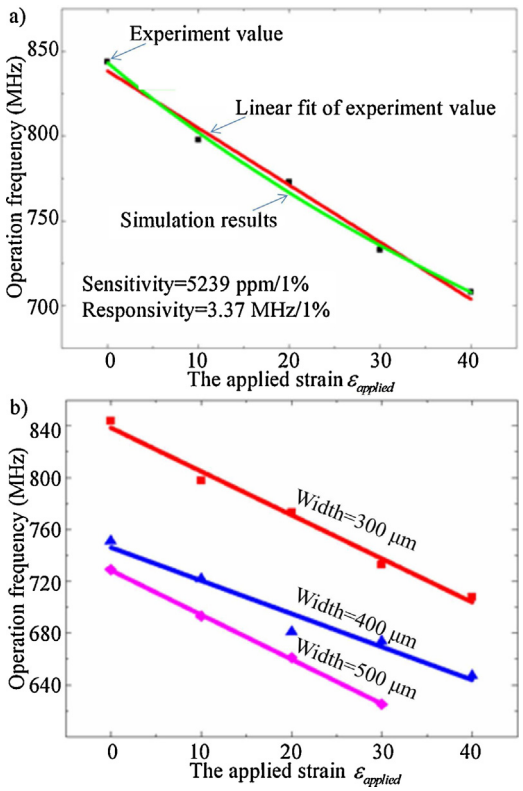

Fig. 10. (a) Measurement results from the sensors with variable inductance designs and sensitivity analysis and (b) resonance frequency versus strain with different line widths.

wireless strain sensing in the variable inductor design. Giving one strain of the wireless strain sensor, working frequency point can be detected through the external coil linked to vector network analyzer. From the resonance frequency, one can compute strain status of the wireless sensor.

Fig. 10a shows the relationship between the applied strain and the corresponding resonance frequency of self-similar antenna with $w_{line} = 300$ μm. A linear fitting curve can well depict the relationship between operation frequency and the applied strain, as the solid red line. Theoretical computation results of Eq. (4) agree well with the experiment data. The stretchable sensors based on self-similar antenna achieved excellent strain sensing performance (with high responsivity 33.7 MHz/10%), providing readouts with resolutions smaller than 10% so as to sufficiently cover all strain variations of the practical skin monitoring. Highly sensitive strain responses are obtained based on the high compliance of the flexible diaphragm and high resonance frequency. Fig. 10b shows the resonant working frequency of fractal coil with width of 300, 400 and 500 μm. All these results show significantly linear relationship between the resonance frequency and the applied strain. The width of the self-similar structures plays a critical role in the stretchability of fractal antenna, and determines the resonance frequency, but has no influence on the sensitivity. The self-similar antenna with $w_{line} = 500$ μm width is broken when stretched up to 40%, so we cannot get the corresponding operation frequency.

6. Conclusions

We have presented a stretchable wireless strain sensor with a fractal coil which is with a novel self-similar structure, and the complete design, fabrication, characterization and sensitivity analysis are described in detail. The self-similar serpentine structure was utilized to satisfy the requirement of large deformation in stretchable sensor, and it can satisfy low stiffness comparable with soft materials such as skin, in addition to large deformability. FEA results illustrated the large deformation of the fractal coil, and it agrees well with experiment results. Wet etching process is used to fabricate the wireless coil based on Cu film, and it can provide high electrical performances. Influence of resistance R_S, inductance L_S and capacitance C_S has been studied to discover the relationship with the resonance frequency. The wireless strain sensor shows a highly responsivity 33.7 MHz/10%. It can be utilized for long-term continuous skin monitoring onto artificial skin. Future work will be focused on improving the sensing distance of these wireless strain sensors for practical applications.

Acknowledgments

The authors acknowledge supports from the National Natural Science Foundation of China (51322507, 51035002, 51421062) and New Century Excellent Talents in University (NCET-11-0171).

References

[1] D.-H. Kim, N. Lu, R. Ma, Y.-S. Kim, R.-H. Kim, S. Wang, J. Wu, S.M. Won, H. Tao, A. Islam, et al., Epidermal electronics, Science 333 (6044) (2011) 838–843.
[2] M.L. Hammock, A. Chortos, B.C.-K. Tee, J.B.-H. Tok, Z. Bao, 25th anniversary article: the evolution of electronic skin (e-skin): a brief history, design considerations, and recent progress, Adv. Mater. 25 (42) (2013) 5997–6038.
[3] S. Cheng, Z. Wu, Microfluidic stretchable RF electronics, Lab Chip 10 (23) (2010) 3227–3234.
[4] C. Hautamaki, L. Cao, J. Zhou, S.C. Mantell, T.S. Kim, Calibration of MEMS strain sensors fabricated on silicon: theory and experiments, J. Microelectromech. Syst. 12 (5) (2003) 720–727.
[5] N.-K. Chang, C.-C. Su, S.-H. Chang, Fabrication of single-walled carbon nanotube flexible strain sensors with high sensitivity, Appl. Phys. Lett. 92 (6) (2008) 063501.
[6] N. Lu, C. Lu, S. Yang, J. Rogers, Highly sensitive skin-mountable strain gauges based entirely on elastomers, Adv. Funct. Mater. 22 (19) (2012) 4044–4050.
[7] Y. Jeon, R. Sood, J.-H. Jeong, S.-G. Kim, MEMS power generator with transverse mode thin film PZT, Sens. Actuators A: Phys. 122 (1) (2005) 16–22.
[8] X. Xiao, L. Yuan, J. Zhong, T. Ding, Y. Liu, Z. Cai, Y. Rong, H. Han, J. Zhou, Z.L. Wang, High-strain sensors based on ZnO nanowire/polystyrene hybridized flexible films, Adv. Mater. 23 (45) (2011) 5440–5444.
[9] Y. Duan, Y. Huang, Z. Yin, N. Bu, W. Dong, Non-wrinkled, highly stretchable piezoelectric devices by electrohydrodynamic direct-writing, Nanoscale 6 (6) (2013) 3289–3295.
[10] Z. Liu, C. Pan, L. Lin, J. Huang, Z. Ou, Direct-write PVDF nonwoven fiber fabric energy harvesters via the hollow cylindrical near-field electrospinning process, Smart Mater. Struct. 23 (2) (2014) 025003.
[11] A. Daliri, A. Galehdar, S. John, C.H. Wang, W.S. Rowe, K. Ghorbani, Wireless strain measurement using circular microstrip patch antennas, Sens. Actuators A: Phys. 184 (2012) 86–92.
[12] B. Hu, W. Chen, J. Zhou, High performance flexible sensor based on inorganic nanomaterials, Sens. Actuators B: Chem. 176 (2013) 522–533.
[13] F. Wang, O. Hansen, Electrostatic energy harvesting device with out-of-the-plane gap closing scheme, Sens. Actuators A: Phys. 211 (2014) 131–137.
[14] T. Sekitani, M. Takamiya, Y. Noguchi, S. Nakano, Y. Kato, T. Sakurai, T. Someya, A large-area wireless power-transmission sheet using printed organic transistors and plastic MEMS switches, Nat. Mater. 6 (6) (2007) 413–417.
[15] L.A. Gupta, L. Young, B. Wondimu, D. Peroulis, Wireless temperature sensor for mechanical face seals using permanent magnets, Sens. Actuators A: Phys. 203 (2013) 369–372.
[16] A. Ibrahim, D. Cumming, Passive single chip wireless microwave pressure sensor, Sens. Actuators A: Phys. 165 (2) (2011) 200–206.
[17] S. Cheng, Z. Wu, A microfluidic, reversibly stretchable, large-area wireless strain sensor, Adv. Funct. Mater. 21 (12) (2011) 2282–2290.
[18] W. Mokwa, U. Schnakenberg, Micro-transponder systems for medical applications, IEEE Trans. Instrum. Meas. 50 (6) (2001) 1551–1555.
[19] S.-W. Hwang, X. Huang, J.-H. Seo, J.-K. Song, S. Kim, S. Hage-Ali, H.-J. Chung, H. Tao, F.G. Omenetto, Z. Ma, et al., Materials for bioresorbable radio frequency electronics, Adv. Mater. 25 (26) (2013) 3526–3531.
[20] O. Akar, T. Akin, K. Najafi, A wireless batch sealed absolute capacitive pressure sensor, Sens. Actuators A: Phys. 95 (1) (2001) 29–38.
[21] T. Kaiser, et al., Passive telemetric readout system, IEEE Sens. J. 6 (5) (2006) 1340–1345.
[22] C.C. Collins, Miniature passive pressure transensor for implanting in the eye, IEEE Trans. Biomed. Eng. (2) (1967) 74–83.
[23] L. Rosengren, P. Rangsten, Y. Bäcklund, B. Hök, B. Svedbergh, G. Selén, A system for passive implantable pressure sensors, Sens. Actuators A: Phys. 43 (1) (1994) 55–58.

[24] P.-J. Chen, D.C. Rodger, S. Saati, M.S. Humayun, Y.-C. Tai, Microfabricated implantable parylene-based wireless passive intraocular pressure sensors, J. Microelectromech. Syst. 17 (6) (2008) 1342–1351.
[25] N. Xue, S.-P. Chang, J.-B. Lee, A su-8-based microfabricated implantable inductively coupled passive RF wireless intraocular pressure sensor, J. Microelectromech. Syst. 21 (6) (2012) 1338–1346.
[26] B. Kang, H. Hwang, S.H. Lee, J.Y. Kang, J.-H. Park, C. Seo, C. Park, A wireless intraocular pressure sensor with variable inductance using a ferrite material, J. Semicond. Sci. Technol. 13 (4) (2013) 355–360.
[27] X. Huang, Y. Liu, H. Cheng, W.-J. Shin, J.A. Fan, Z. Liu, C.-J. Lu, G.-W. Kong, K. Chen, D. Patnaik, et al., Materials and designs for wireless epidermal sensors of hydration and strain, Adv. Funct. Mater. 24 (25) (2014) 3845.
[28] Y. Huang, Z. Yin, Y. Xiong, Thermomechanical analysis of thin films on temperature-dependent elastomeric substrates in flexible heterogeneous electronics, Thin Solid Films 518 (6) (2010) 1698–1702.
[29] D.-H. Kim, J.-H. Ahn, W.M. Choi, H.-S. Kim, T.-H. Kim, J. Song, Y.Y. Huang, Z. Liu, C. Lu, J.A. Rogers, Stretchable and foldable silicon integrated circuits, Science 320 (5875) (2008) 507–511.
[30] Y. Su, J. Wu, Z. Fan, K.-C. Hwang, J. Song, Y. Huang, J.A. Rogers, Postbuckling analysis and its application to stretchable electronics, J. Mech. Phys. Solids 60 (3) (2012) 487–508.
[31] R.-H. Kim, H. Tao, T.-I. Kim, Y. Zhang, S. Kim, B. Panilaitis, M. Yang, D.-H. Kim, Y.H. Jung, B.H. Kim, et al., Materials and designs for wirelessly powered implantable light-emitting systems, Small 8 (18) (2012) 2812–2818.
[32] N.A. Murad, M. Esa, M.F.M. Yusoff, S.H.A. Ali, Hilbert curve fractal antenna for RFID application, in: IEEE International RF and Microwave Conference, 2006, IEEE, 2006, pp. 182–186.
[33] J.A. Fan, W.-H. Yeo, Y. Su, Y. Hattori, W. Lee, S.-Y. Jung, Y. Zhang, Z. Liu, H. Cheng, L. Falgout, et al., Fractal design concepts for stretchable electronics, Nat. Commun. 5 (2014).
[34] S. Xu, Y. Zhang, J. Cho, J. Lee, X. Huang, L. Jia, J.A. Fan, Y. Su, J. Su, H. Zhang, et al., Stretchable batteries with self-similar serpentine interconnects and integrated wireless recharging systems, Nat. Commun. 4 (2013) 1543.
[35] A. Grosse, M. Grewe, H. Fouckhardt, Deep wet etching of fused silica glass for hollow capillary optical leaky waveguides in microfluidic devices, J. Micromech. Microeng. 11 (3) (2001) 257.
[36] Y. Zhang, H. Fu, S. Xu, J.A. Fan, K.-C. Hwang, J. Jiang, J.A. Rogers, Y. Huang, A hierarchical computational model for stretchable interconnects with fractal-inspired designs, J. Mech. Phys. Solids 72 (2014) 115–130.
[37] Y. Zhang, H. Fu, Y. Su, S. Xu, H. Cheng, J.A. Fan, K.-C. Hwang, J.A. Rogers, Y. Huang, Mechanics of ultra-stretchable self-similar serpentine interconnects, Acta Mater. 61 (20) (2013) 7816–7827.
[38] P.-J. Chen, S. Saati, R. Varma, M.S. Humayun, Y.-C. Tai, Wireless intraocular pressure sensing using microfabricated minimally invasive flexible-coiled LC sensor implant, J. Microelectromech. Syst. 19 (4) (2010) 721–734.

Biographies

YongAn Huang received the B.S. and M.S. degrees in civil engineering and the Ph.D. degree in engineering mechanics from Northwestern Polytechnical University, Xi'an, China, in 2001, 2004, and 2007, respectively. He was a Post-Doctoral Fellow with the School of Mechanical Science and Engineering, Huazhong University of Science and Technology, Wuhan, China, in 2007, where he is currently an Associate Professor with the State Key Laboratory of Digital Manufacturing Equipment and Technology.
His current research interests include flexible electronics manufacturing and advanced material and structural mechanics.
Dr. Huang was a recipient of the China National Funds for Excellent Young Scientists Award.

Wentao Dong received the B.S. and M.S. degrees in mechanical engineering from Wuhan University of Technology, Wuhan, China, in 2009 and 2012, respectively. He is currently pursuing the Ph.D. degree in mechanical engineering with the School of Mechanical Science and Engineering, Huazhong University of Science and Technology (HUST), Wuhan, China.
He is with the State Key Laboratory of Digital Manufacturing Equipment and Technology at HUST. His current research interests include flexible and stretchable electronic device manufacture and application.

Tao Huang received the B.S. degree in mechanical engineering from Wuhan University of Technology, Wuhan, China, in 2013. He is currently pursuing the M.S. degree in mechanical engineering with the School of Mechanical Science and Engineering, Huazhong University of Science and Technology (HUST), Wuhan, China.
He is with the State Key Laboratory of Digital Manufacturing Equipment and Technology at HUST. His current research interests include design and fabrication of flexible electronic device.

Yezhou Wang received the B.S. degree in Electronic Packaging Technology from Huazhong University of Science and Technology (HUST), Wuhan, China, in 2013. He is currently pursuing the M.S. degree in mechanical engineering with the School of Mechanical Science and Engineering, Huazhong University of Science and Technology (HUST), Wuhan, China.
He is with the State Key Laboratory of Digital Manufacturing Equipment and Technology at HUST. His current research interests include microfliud eletronic device.

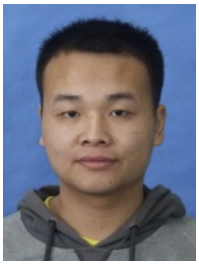

Lin Xiao received the B.S. degree in engineering mechanics from Huazhong University of Science and Technology (HUST), Wuhan, China, in 2014. He is currently pursuing the Ph.D. degree in mechanical engineering with the School of Mechanical Science and Engineering, Huazhong University of Science and Technology (HUST), Wuhan, China.
He is with the State Key Laboratory of Digital Manufacturing Equipment and Technology at HUST. His current research interests include feature mechanics and flexible display application.

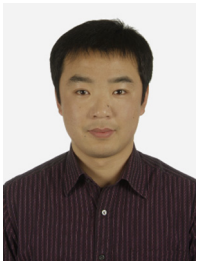

Yewang Su received the B.S. degree in Engineering Mechanics from Dalian University of Technology, Dalian, China, in 2005. He received the M.E. and Ph.D. degrees in engineering mechanics from Tsinghua University, Beijing, China, in 2007 and 2011, respectively. He was a Post-Doctoral Fellow (w/ Prof. Yonggang Huang) with Departments of Civil and Environmental Engineering and Mechanical Engineering, Northwestern University, Evanston, IL, US, from 2011.3 to 2014.1. He was a Post-Doctoral Fellow (w/ Prof. Zdeněk P. Bažant) with Departments of Civil and Environmental Engineering, Northwestern University, Evanston, IL, US, from 2014.2 to 2014.11, where he is currently a Research assistant professor with Departments of Civil and Environmental Engineering, Northwestern University from 2014.12.
His current research interests include Gas shale, Stretchable electronics and Biomechanics.

Zhouping Yin received the B.S. and Ph.D. degrees in mechanical engineering from the Huazhong University of Science and Technology (HUST), Wuhan, China, in 1994 and 2000, respectively.
He is a Distinguished Professor, and has been the Vice Head of the State Key Laboratory of Digital Manufacturing Equipment and Technology, HUST, since 2005. He is a Principal Investigator for projects sponsored by the General Program and Major Program of the National Science Foundation, National Basic Research Project of China. He is leading a research group and conducting research in electronic manufacturing equipment and technology, including printed electronics and radio frequency identification packaging.
Dr. Yin is a member of the Chang Jiang Scholars Program. He was a recipient of the China National Funds for Distinguished Young Scientists Award.